Available online at www.sciencedirect.com

ScienceDirect

Mendeleev Commun., 2023, **33**, 343–345

Mendeleev Communications

Synthesis and bioimaging application of red-emissive carbon dots

Feng Yu,[a] Menghui Ma,[a] Xiaoyan Wu,[b] Zijian Li[b] and Hong Bi*[b]

[a] *School of Chemistry and Chemical Engineering, Anhui University, 230601 Hefei, China*
[b] *School of Materials Science and Engineering, Anhui University, 230601 Hefei, China. Fax: +86 551 63861279; e-mail: bihong@ahu.edu.cn*

DOI: 10.1016/j.mencom.2023.04.015

Fluorescent red-emissive carbon dots (RCDs) were synthesized using the solvothermal method with citric acid as a carbon source, *N*,*N*-dimethylformamide as a nitrogen source, and formamide as a solvent. The as-synthesized RCDs show red fluorescence in an aqueous solution and have an excellent stability towards photobleaching as well as extremely low cytotoxicity and are successfully used for cell and zebrafish imaging. The results indicate that RCDs have potential applications in both *in vitro* and *in vivo* bioimaging.

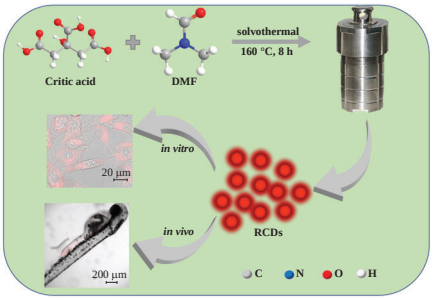

Keywords: carbon dots, red emission, bioimaging, zebrafish, nitrogen-doped.

Common conventional fluorescent materials include organic fluorescent dyes and semiconductor quantum dots, which pose obvious hazards to the environment and human health. In contrast, carbon dots (CDs), as a novel fluorescent material, have become a focus of research due to their low toxicity, high fluorescence stability, high water solubility, and easy functionalization.[1,2] Carbon dots have great potential for applications in many fields such as bioimaging and drug release,[3] tunable optical performance,[4] optical electronics,[5] and ion detection.[6] Most of the reported CDs usually have strong emission located in the short-wavelength region (*e.g.*, blue and green emission regions).[7] In contrast, CDs with long-emission wavelengths are rare and have low fluorescence.[8] Carbon dots with short-wavelength emissions are highly limited in bioimaging. Therefore, there is a great need to prepare long-wavelength emitting CDs by simple and green methods.

The optical properties of CDs can be changed by various methods, such as surface passivation, heterogeneous atom doping, and particle size changing.[9–11] For example, Yang *et al.*[12] successfully synthesized N-doped CDs with emission in the red spectral range by the hydrothermal method using *o*-phenylenediamine as a carbon source and precursor. In addition, the CDs were used as fluorescent probes for cells and mice *in vivo*. Various characterization methods confirmed that the red emission is due to the large size effect caused by the large aromatic π-conjugated structure and hydrogen bonding. A new idea was provided for the exploration of CD photoluminescence. In 2020, Su *et al.*[13] used citric acid and urea to synthesize nitrogen-rich CDs by the solvothermal method. The obtained CDs were modified with surface charge engineering (treatment with sodium hydroxide and hydrochloric acid solutions) to give them red light emitting properties with a single emission center and optical characteristics depending on the excitation wavelength. The maximum emission wavelength was 605 nm with excitation at 555 nm. The powder XRD pattern obtained for these CDs corresponds to (002) planes of the graphitic structure, indicating highly conjugated sp^2 domains in the core of CDs occupying the main position. Compared to other methods, heteroatom doping is less likely to form polymer impurities during synthesis,[14] and the functional groups formed on the surface of CDs can significantly alter their luminescence properties. Heteroatom doping is commonly used to modify the photoluminescence of CDs. It has been shown that many atoms such as N, P, S, B and Se can effectively increase the fluorescent ability and efficiency of CDs. Nitrogen atoms behave more effectively among these atoms. Therefore, a lot of N-doped CDs have been prepared and successfully applied in many fields such as bioimaging and therapy, photocatalysis, ion detection, and optical electronic parts. Jiang *et al.*[15] successfully synthesized the F, N-doped CDs (N-CDs-F) with a UV–VIS–NIR full-range response, which were produced by the solvothermal method using urea citrate with the aid of ammonium fluoride, and their multiphoton absorption cross section was larger than that of F, N-doped CDs obtained from conventional organic compounds with a NIR emission band centered at 777 nm at ~700 nm excitation.

In this study, we report a green method for the preparation of red-emissive CDs (RCDs) which were prepared by the one-pot solvothermal method using citric acid and DMF as precursors. The morphology of the products was determined by transmission electron microscopy (TEM). The elemental composition and surface structure of RCDs were examined by Fourier transform infrared (FTIR) spectroscopy and X-ray photoelectron spectroscopy (XPS). The structure and optical properties of RCDs were investigated by UV–VIS absorption spectroscopy and fluorescence emission spectroscopy. In addition, RCDs have excellent biocompatibility and have been successfully used for bioimaging of zebrafish.

The RCDs were synthesized by the one-step solvothermal method and the yield of the RCDs prepared from the bulk material was 19%. The morphology of the RCDs was characterized using transmission electron microscopy. The TEM image [Figure 1(*a*)] shows that the prepared RCDs are spherical and well separated from each other, and the inset high-resolution TEM (HRTEM) image demonstrates lattice fringes of a single

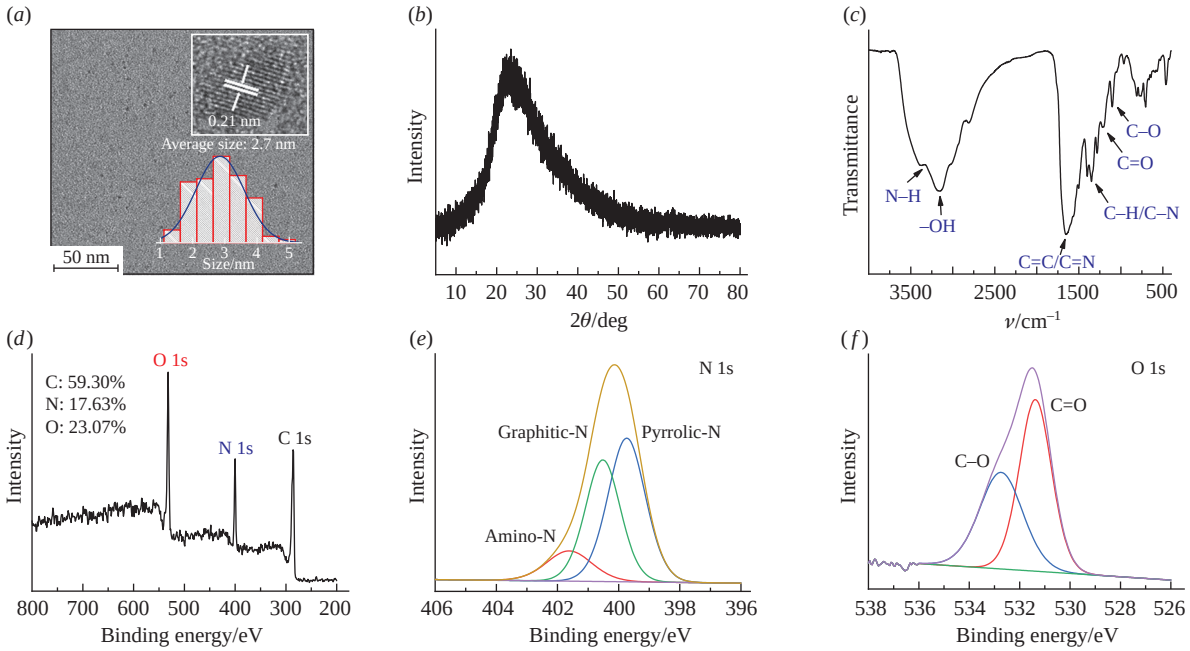

Figure 1 (*a*) TEM, HRTEM (inset) images, and size distribution (inset); (*b*) XRD pattern; (*c*) FTIR spectrum; (*d*) XPS survey spectrum; and high-resolution (*e*) N 1s and (*f*) O 1s XPS spectra of the RCDs.

carbon dot with a typical interplanar spacing (*d*-spacing) of 0.21 nm ascribed to that of the (100) facet of graphitic carbon.[15] Another inset in Figure 1(*a*) shows the corresponding size distribution histogram indicating the particle diameters of the prepared RCDs ranging from 2.3 to 4.4 nm with an average diameter of 2.7 nm. As shown in Figure 1(*b*), a wide diffraction peak can be observed at 23°. The chemical structures of the RCDs were further characterized using FTIR and XPS. The FTIR spectra of the RCDs [Figure 1(*c*)] showed the peaks near 3428 cm^{-1} belonging to N–H and O–H stretching vibrational peaks, indicating the presence of hydroxyl and amino groups. There is a peak of C=C/C=N stretching vibration near 1660 cm^{-1}, while the characteristic absorption at 1353 cm^{-1} was assigned to C–H/C–N stretching, and the peak at 1276 cm^{-1} belongs to C=O vibrations. In addition, the peak at 1109 cm^{-1} is attributed to the bending vibration of the C–O bond in the carboxyl group. We further demonstrated the elemental and structural composition of the RCDs based on XPS. The full XPS [Figure 1(*d*)] proved that the RCDs were composed of the elements C 1s (286.18 eV, 59.30%), O 1s (532.56 eV, 23.07%), and N 1s (400.96 eV, 17.63%). The high-resolution N 1s spectrum [Figure 1(*e*)] consists of two strong single peaks at 399.6 eV, 400.5 eV and a weak peak at 401.4 eV, which were ascribed to pyrrolic-N, graphitic-N, and amino-N, respectively. Oxygen [Figure 1(*f*)] is present in the form of carbonyl or carboxyl groups as well as hydroxyl and ester groups. This also corresponds to the results of the ^{1}H NMR (Figure S1, see Online Supplementary Materials).

Figure 2 shows UV–VIS absorption spectra, optimal fluorescence excitation spectra, and emission spectra of the RCDs. As shown in Figure 2(*a*), the peak at 220–270 nm corresponds to the π–π* transition in aromatic rings, and the peak at 530 nm corresponds to the n–π* transition of π-systems containing C–N/C=N bonds. The latter peak is responsible for the luminescence at 630 nm. When the excitation wavelength shifts from 350 to 570 nm, the emission wavelength is gradually red shifted [Figure 2(*b*)]. At 530 nm excitation, the optimal emission at 630 nm was obtained. The time-resolved photoluminescence (PL) spectra of the RCDs exhibited a fast PL decay with an average lifetime of 2.05 ns (Figure S2, see Online Supplementary Materials), revealing the CDs' common fluorescence nature with a short lifetime. Interestingly, we found that the RCDs show different optical behavior in different solvents. The UV–VIS absorption and PL spectra in the following three different polar solvents such as water, formamide, and dimethyl sulfoxide (DMSO) were implemented. These dispersions exhibit homogeneous phases without any obvious precipitation at room temperature. Figure 2(*c*) shows the normalized fluorescence emission spectrum of the RCDs individually dispersed in three solvents, the optimum fluorescence emission wavelength gradually red shifts from 630 to 640 nm, and the corresponding UV–VIS absorption peak also gradually shifts from 530 to 590 nm. Solvent polarity highly affects the PL emission wavelength of CDs. The RCDs show solvent-dependent behavior. As expected, the RCDs show a negative zeta potential [−3.74 mV, Figure S3(*a*), see Online

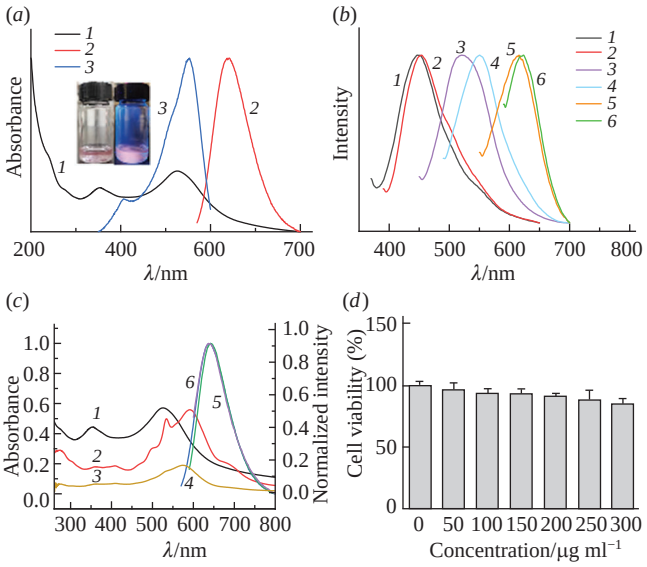

Figure 2 (*a*) UV–VIS absorption and the corresponding PL emission and PL excitation (PLE) spectra of the RCDs in water and its appearance under (left inset) visible and (right inset) UV light; (*b*) luminescence spectra obtained by excitation at 350–570 nm; (*c*) UV–VIS absorption spectra in (*1*) H_2O, (*2*) formamide, and (*3*) DMSO at room temperature and the normalized fluorescence spectra of the RCDs in (*4*) H_2O, (*5*) formamide, and (*6*) DMSO; and (*d*) MTT results of HepG2 cells co-incubated with various concentrations of the RCDs, $n = 3$.

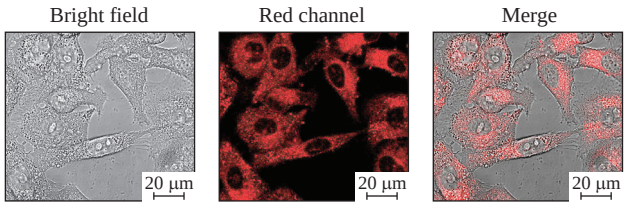

Figure 3 CLSM images of HepG2 cells co-incubated with 300 μg ml^{-1} RCDs under 561 nm excitation.

Supplementary Materials] and an average hydrodynamic diameter of 79.72 nm measured by dynamic laser scattering (DLS), as shown in Figure S3(*b*) (see Online Supplementary Materials).

A possible mechanism for the luminescence of the RCDs is that the π–π conjugated aromatic structure would consequently lower the energy gap by increasing the size of the sp^2 domain, thus resulting in the emission of red luminescence. On the other hand, the N-containing groups (graphitic-N, pyrrolic-N, and amino-N) provide surface molecular state-related fluorescence.

Classical MTT assay was used to evaluate the cytotoxicity of the RCDs. The MTT results [Figure 2(*d*)] indicate an extremely low cytotoxicity because the cell viability rate can reach more than 80% even when the concentration of the RCDs reaches as high as 300 μg ml^{-1}.

Figure 3 shows the usage of the RCDs for cell imaging. Specifically, the fluorescence confocal laser scanning microscopy (CLSM) images in Figure 3 were recorded after HepG2 cells were incubated with the RCDs for 4 h and subsequently washed. The microscopy images show the accumulation of the RCDs on the cells, clearly showing their contours. Figure S4(*a*) (see Online Supplementary Materials) shows images of zebrafish embryos incubated with 300 μg ml^{-1} RCDs for 2 and 96 h. The fluorescence imaging of samples in the zebrafish was assessed by analyzing transparent zebrafish embryos and larval stages. After 4 h of co-incubation with 300 μg ml^{-1} RCDs, the embryos showed fluorescent signals [Figure S4(*b*)] (see Online Supplementary Materials), which correspond to their entry through the chorion. After 96 h, the RCDs accumulated in the digestive system of the zebrafish larvae. These results indicate that RCDs have specific biomedical potential.

In summary, we have synthesized red-emissive, water-soluble and low-cytotoxic carbon dots (RCDs) by a simple solvothermal method. The as-synthesized RCDs can be used for bioimaging of cells and organelles of zebrafish.

This work was financially supported by the National Natural Science Foundations of China (grant nos. 52172033, 22005280) and the Anhui Province Key Research and Development Plan Project International Science and Technology Cooperation Special Project (no. 202004b11020015). We acknowledge the support of the Key Laboratory of Structure and Functional Regulation of Hybrid Materials of Ministry of Education, Anhui University, Hefei, Anhui 230601, China. We also acknowledge support of the Key Laboratory of Environment Friendly Polymer Materials of Anhui Province, Hefei, China and Key Laboratory of Functional Inorganic Material Chemistry of Anhui Province, Anhui University, Hefei 230601, P. R. China.

Online Supplementary Materials

Supplementary data associated with this article can be found in the online version at doi: 10.1016/j.mencom.2023.04.015.

References

1 S. Zhu, X. Zhao, Y. Song, S. Lu and B. Yang, *Nano Today*, 2016, **11**, 128.
2 C. Shen, J. Wang, Y. Cao and Y. Lu, *J. Mater. Chem. C*, 2015, **3**, 6668.
3 M.-J. Youh, M.-C. Chung, H.-C. Tai, C.-Y. Chen and Y.-Y. Li, *Mendeleev Commun.*, 2021, **31**, 647.
4 J. Xu, Q. Liang, Z. Li, V. Yu. Osipov, Y. Lin, B. Ge, Q. Xu, J. Zhu and H. Bi, *Adv. Mater.*, 2022, **34**, 2200011.
5 B. Wang, J. Li, Z. Tang, B. Yang and S. Lu, *Sci. Bull.*, 2019, **64**, 1285.
6 R. Wang, X. Wang and Y. Sun, *Sens. Actuators, B*, 2017, **241**, 73.
7 X. Wei, L. Li, J. Liu, L. Yu, H. Li, F. Cheng, X. Yi, J. He and B. Li, *ACS Appl. Mater. Interfaces*, 2019, **11**, 9832.
8 D. Li, P. Jing, L. Sun, Y. An, X. Shan, X. Lu, D. Zhou, D. Han, D. Shen, Y. Zhai, S. Qu, R. Zbořil and A. L. Rogach, *Adv. Mater.*, 2018, **30**, 1705913.
9 R. Guo, L. Li, B. Wang, Y. Xiang, G. Zou, Y. Zhu, H. Hou and X. Ji, *Energy Storage Mater.*, 2021, **37**, 8.
10 H. Ding, S.-B. Yu, J.-S. Wei and H.-M. Xiong, *ACS Nano*, 2016, **10**, 484.
11 J. Bai, Y. Ma, G. Yuan, X. Chen, J. Mei, L. Zhang and L. Ren, *J. Mater. Chem. C*, 2019, **7**, 9709.
12 J. Liu, D. Li, K. Zhang, M. Yang, H. Sun and B. Yang, *Small*, 2018, **14**, 1703919.
13 D. Su, X. Han, X. Yan, R. Jin, H. Li, D. Kong, H. Gao, F. Liu, P. Sun and G. Lu, *Anal. Chem*., 2020, **92**, 12716.
14 H. Nie, M. Li, Q. Li, S. Liang, Y. Tan, L. Sheng, W. Shi and S. X.-A. Zhang, *Chem. Mater.*, 2014, **26**, 3104.
15 L. Jiang, H. Ding, M. Xu, X. Hu, S. Li, M. Zhang, Q. Zhang, Q. Wang, S. Lu, Y. Tian and H. Bi, *Small*, 2020, **16**, 2000680.

Received: 7th November 2022; Com. 22/7041